

SPREADING DYNAMICS WITH LATTICE BOLTZMANN METHOD

Felipe Reinoldo Schramm

Federal University of Santa Catarina - Florianópolis - Santa Catarina - Brazil
Schramm@lmpt.ufsc.br

Fabiano G. Wolf

Federal University of Santa Catarina - Florianópolis - Santa Catarina - Brazil
fgwolf@lmpt.ufsc.br

Luís Orlando Emerich dos Santos

Federal University of Santa Catarina - Florianópolis - Santa Catarina - Brazil
emerich@lmpt.ufsc.br

Paulo Cesar Philippi

Federal University of Santa Catarina - Florianópolis - Santa Catarina - Brazil
philippi@lmpt.ufsc.br

Abstract. *The Lattice Boltzmann method has been applied with relative success to simulate fluid flows in porous media, phase transitions and interfacial phenomena. In this work, droplet spreading dynamics in homogeneous and heterogeneous surfaces is studied using the Immiscible Lattice Boltzmann based on field mediators. This method permits to simulate immiscible fluid dynamics and the interaction of the fluids with the solid surface. The results of simulations are compared with published experimental data.*

Keywords: *Spreading dynamics, Immiscible lattice Boltzmann method*

1. Introduction

The study of surface phenomena problems, i.e., in which different fluids can interact with a solid substrate, was always subject of great scientific and economical interest. One commonly studied phenomena is the surfaces wettability. It happens due to the intermolecular forces action among the both fluids molecules and the solid ones and results in the macroscopic contact angle, usually defined through the Young-Dupré equation. In what refers to contact line dynamics, it is known that the three phases simultaneous interaction in the contact line area influences directly static and dynamics of wettability (Dussan, 1979). However, it is not known the precise mechanism for contact line movement through the solid surface and how that mechanism interacts with the rest drainage (Blake and Coninck, 2002). Even Young-Dupré equation - that describes the thermodynamic balance characterized by a certain contact angle - has its validity questioned (Liu and German, 1996). In order to study the wettability phenomena, the Immiscible Lattice Boltzmann (ILB) model, developed by Santos, Facin and Philippi (2003), was used to simulate droplet spreading dynamics on solid surfaces with different wettability conditions. In this way, the chemical heterogeneities influence on contact line dynamics can be observed.

2. Lattice Boltzmann Method

The Lattice Boltzmann Method (LBM) can be regarded as a discrete counterpart of the Boltzmann's transport equation, in which space and velocities can assume only discrete values. The continuous space is replaced by the vertices of a regular lattice, named lattice sites. Each site is characterized by a particle distribution function $N_i(\mathbf{X}, T)$ which evolves according to the Lattice Boltzmann Equation:

$$N_i(\mathbf{X} + \mathbf{c}_i, T + 1) = N_i(\mathbf{X}, T) + \Omega_i, \quad (1)$$

where T is the time variable, the index i indicates the neighbor, \mathbf{c}_i is a velocity vector pointing to neighbor i ($i = 0$ refers to the rest particle distribution). The term in the right side is called collision operator and is written in such way that

$$\sum_i \Omega_i = 0, \quad (2)$$

$$\sum_i \Omega_i \mathbf{c}_i = 0, \quad (3)$$

in order to preserve the mass and momentum of each site.

The evolution of the model, given by Eq. (1), can be split in two processes. In the first, designated as collision, the distribution function $N_i(\mathbf{X}, T)$ is changed by the action of the collision operator. In the second process, called

propagation, the values N_i are propagated to the neighboring sites, in accordance with the direction of the vector c_i . The mass and momentum variables are defined with the help of the distribution function:

$$\sum_{i=0}^b N_i = \rho, \quad (4)$$

$$\sum_{i=0}^b N_i \mathbf{c}_i = \rho \mathbf{u}. \quad (5)$$

Usually, a single relaxation time approximation for the collision is used (see Qian et al., 1992):

$$\Omega_i = \frac{N_i^{eq} - N_i}{\tau}, \quad (6)$$

where T is the relaxation time and N_i^{eq} is called equilibrium distribution.

With a suitable choice of the equilibrium distribution it can be shown that the model evolves according to following equations:

$$\partial_t(\rho) + \partial_\beta(\rho u_\beta) = 0, \quad (7)$$

$$\partial_t(\rho u_\alpha) + \partial_\beta(\rho u_\alpha u_\beta) = -\partial_\alpha(p) + \nu \partial_\beta [\partial_\beta(\rho u_\alpha) + \partial_\alpha(\rho u_\beta)], \quad (8)$$

where the pressure p and the kinematic viscosity ν are given by

$$p = \frac{1}{3}\rho, \quad (9)$$

$$\nu = \frac{1}{3}(\tau - 1/2). \quad (10)$$

The mass balance equation is, exactly, the same equation obtained in classical hydrodynamics. Considering low Mach number (p constant), the obtained momentum balance equation will be, clearly, in agreement with the Navier-Stokes equation.

3. Immiscible Lattice Boltzmann

In this work, a lattice-Boltzmann model based on field mediators was employed. The model is fully described in Santos, Facin and Philippi (2003), and some slight improvements commented at the end of present section, were performed. Two particle distribution functions, R_i and B_i , are used to describe the immiscible fluids r and b . Particles interaction is modeled by splitting the BGK collision term, considering, separately, r - r and r - b collisions. A third distribution function – namely, the mediator's distribution function M_i – is used to model the long range interaction, carrying out neighborhood information. The distribution functions are updated considering two steps:

- a) a *local step* – involving the particles collision process and the emission/ annihilation of the field mediators;
- b) a *non-local step*, i.e., the propagation step.

In what follows, \mathbf{X} is the position vector and \mathbf{c}_i is a discrete velocity. In the local step particle distributions are updated at each time step T by a collision process:

$$R'_i = R_i + \omega^r \frac{R_i^0(\rho^r, \mathbf{u}^r) - R_i}{\tau^{rr}} + \omega^b \frac{R_i^0(\rho^r, \vec{\vartheta}^b) - R_i}{\tau^m}, \quad (11)$$

$$B'_i = B_i + \omega^b \frac{B_i^0(\rho^b, \mathbf{u}^b) - B_i}{\tau^{bb}} + \omega^r \frac{B_i^0(\rho^b, \vec{\vartheta}^r) - B_i}{\tau^m}, \quad (12)$$

where

$$\rho^k = \sum_{i=0}^{b_m} K_i, \quad \mathbf{u}^k = \frac{1}{\rho^k} \sum_{i=1}^{b_m} K_i \mathbf{c}_i, \quad (13)$$

are, respectively, the macroscopic density and the velocity of component k , $k = r, b$. R_i^0 and B_i^0 are the equilibrium distributions. The ω 's are the mass fractions, $\omega^k = \rho^k / \rho$. The ϑ 's are the local velocities modified by the action of mediators,

$$\vec{\vartheta}^r = \mathbf{u}^r + A \hat{\mathbf{u}}^m, \quad \vec{\vartheta}^b = \mathbf{u}^b - A \hat{\mathbf{u}}^m, \quad (14)$$

and

$$\hat{\mathbf{u}}^m = \frac{\sum_i M_i \mathbf{c}_i}{|\sum_i M_i \mathbf{c}_i|}. \quad (15)$$

The mediator's distribution are updated by an *emission/annihilation* step, defined by

$$M'_i = \alpha M_i + \beta \frac{R_i}{R_i + B_i}, \quad (16)$$

where α and β are weights used for settling the interaction length[?]. The propagation step is the only non-local step and is identical for all the distributions,

$$K_i(\mathbf{X} + \mathbf{c}_i, T + 1) = K'_i(\mathbf{X}, T) \quad (17)$$

where $K = R, B$ or M . The model described in this section differs from the model previously proposed in Santos, Facin and Philippi (2003) in two points:

a) A single distribution function is used for describing the distribution of mediators, instead of two, as in the previous model. This modification can be considered as a computational improvement and does not change the theoretical aspects of the model, since, in the previous model, the mediators-particles interaction rules were, effectively, based on the difference between the two distributions.

b) The emission/annihilation step (see Eq. 16) was previously written $M'_i = \alpha M_i^r + \beta w^r$. In our simulations, this change appears to decrease the magnitude of the spurious currents, although a more detailed analysis remains to be done.

3.1 Boundary conditions

At the solid surface, bounce back boundary conditions for the particle distributions were imposed. The boundary conditions for the mediators distribution try to modulate the interaction process between the solid and the fluid. The wettability, or the desired contact angle, can be obtained by imposing, at each fluid site adjacent to a solid site, a constant value M_i^{solid} for the mediator distribution along the directions i leading to the fluid phase in the propagation step. This quantity determines the contact angle, since it determines the interaction between solid and fluids. As the mediator distribution carries the values of mass fraction, $M_i \in [0, 1]$, when $M_i^{solid} = 1/2$ the contact angle will be $\theta = 90^\circ$. When $M_i^{solid} > 1/2$, fluid r will behave as the wetting fluid, and when $M_i^{solid} < 1/2$, fluid b will behave as the wetting fluid. Nevertheless, the precise value of the contact angle also depends on the relaxation parameters (τ_{rr} , τ_{bb} , τ_m).

4. Wettability

In a broad sense, the interaction among two fluids and a solid surface is called wettability. This property is the result of molecular interactions among the molecules of two or more fluids and the molecules of a solid substratum. When two immiscible fluids are in contact with a solid surface, the existence of a common line for the three phases is observed, this line is known as contact line. This situation originates the definition of the contact angle θ , that is, the resulting angle between a tangent line to the interface that separates the immiscible, fluids and the solid surface, as shown at Figure 1.

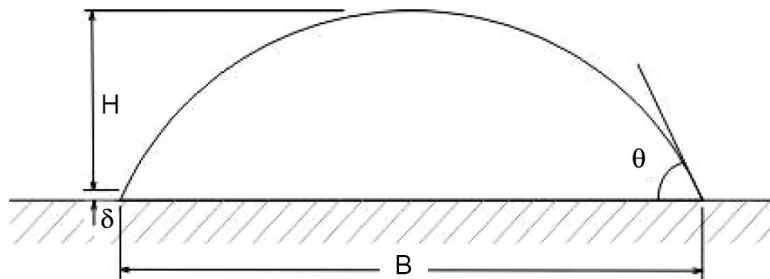


Figure 1. Definition of the contact angle.

4.1 Contact angle determination

Considering the interface as spherical cap (out of gravity action), it can be shown that the contact angle obtained follows the geometric relationship:

$$\theta = 2 \arctan \left(\frac{2H}{B} \right), \quad (18)$$

where H is the drop height and B the contact area diameter between drop and solid. The contact area is not measured close to the surface to avoid the complex region of the contact line. The parameter δ denotes an height above the base, where the diameter B is measured. In this study δ has a value equal to 3 lattice spaces. When a drop is put in contact with a solid surface three different configurations can result: (i) the drop disperses on the surface until an equilibrium contact angle is reached. In this configuration the drop phase is called wetting for that surface ($\theta_e < 90^\circ$); (ii) the drop contracts on the surface until an equilibrium contact angle is reached. In that configuration the drop phase is called not-wetting ($\theta_e > 90^\circ$); (iii) the drop disperses completely, covering the whole surface and forming a fine film of wetting fluid ($\theta = 0^\circ$).

4.2 Experimental evidences in dynamic conditions

A revision of experimental results (for complete wetting) available in literature was given by Marmur (1983). According to the author, the available experimental data for the drops spreading on solid surfaces obeys an empirical relation, given by:

$$R \propto t^n \quad (19)$$

where R is the base drop radius (contact area with the solid), t is the time and n is an empiric coefficient. In agreement with Marmur (1983), it is noticed that the most of values for n are between 0.100 and 0.145, although values of 0.0330 and 0.3135 are also reported (according to Cazabat (1987)). These deviations can be caused by instabilities in contact line, produced by temperature gradients in the liquid (Williams, 1977)).

5. Results and discussion

All simulations in this study were done using periodic boundary conditions, in the absence of gravity. The particles density per site ρ are set equal to 1. The relaxation times (τ_R, τ_B, τ_m) are set 1, resulting in viscosities, $\nu = 1/6$ (in lattice units).

5.1 Spread on homogeneous surfaces

The relationship between interaction factor and contact angle for two-dimensional model is shown in Fig. 2. For three-dimensional simulations the relationship is equivalent (as verified in simulations).

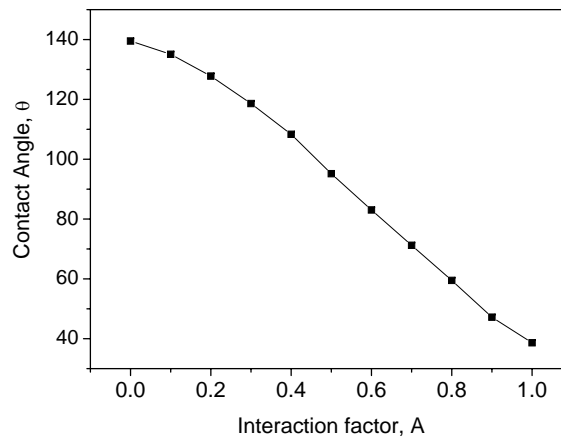


Figure 2. Relationship between interaction factor and contact angle for two-dimensional cases.

5.2 Variation of the exponent n with the initial condition

To verify the model supplied, results agreement with there available in literature, is considered a drop on a flat and homogeneous solid surface, in two different initial conditions: (a) spherical drop and (b) semi-spherical. In both cases, each field of the domain is filled out with only one of fluids. Initially, a sphere with radius equal to 30 lattice sites, composed of R fluid, is generated in the computational domains center. All of the remaining sites are filled out with the B fluid. Some time steps are necessary for the drop become perfectly spherical and stable. The stability condition adopted is $\Delta\rho_R = \rho_R^{t+1} - \rho_R^t < 10^{-5}$. This feels around 120 time steps. Then, the area corresponding to the solid plate is designated as solid in the computational domain. In case (a), the solid area is only a tangent plan to the drop. In case

(b), this area occupies the whole inferior half of the domain, eliminating half drop, and characterizing the initial contact situation. When the drop contacts the solid surface, it disperses or retracts until a characteristic contact angle reaches. This equilibrium contact angle is characteristic of the surface wettability. During the drop spreading, the contact area radius, between drop and solid, is measured. It is assumed here, implicitly, that the circular symmetry is maintained in whole spreading. Taking a central cut in plan zx (or zy), the position of the lattice site that contain the contact line in plan xy can be obtain for the following expression:

$$\mathbf{x}_{int} = \frac{\sum_{x=1}^{nx/2} \mathbf{x} \rho_R \rho_B}{\sum_{x=1}^{nx/2} \mathbf{x} \rho_{R_i} \rho_{B_i}} \quad (20)$$

where ρ_{R_i} and ρ_{B_i} are the fluids R and B densities in the site of position \mathbf{x} . From the contact line position, is determined the contact area radius. Assuming that $R \propto t^n$, the exponent n can be determined from the curve angular coefficient in $\ln R \times \ln t$ graph. Coming this way, it is obtained for case (a) $n = 0.617 \pm 0.00714$, and for case (b) $n = 0.119 \pm 0.000425$ (shown in fig. 4.2). Observing the presented results, it can be noticed that there is a significant variation of n in agreement with the initial system condition. The subsequent analyses are made being considered initial condition same to (b).

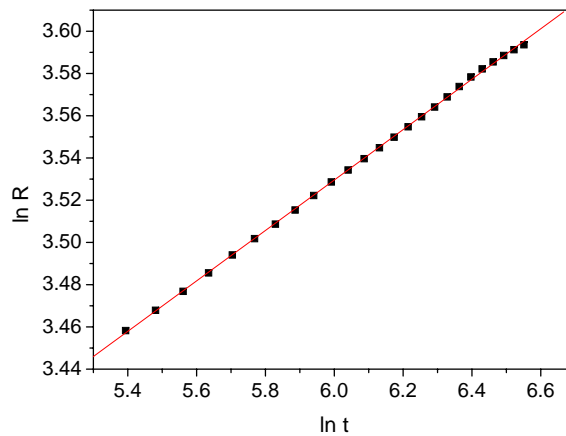


Figure 3. $\ln R \times \ln t$ graph of a drop spreading, in condition (b), on a flat and homogeneous solid surface. In this case, the interaction factor is equal to 0.82, resulting in an angular coefficient of $n = 0.119 \pm 0.000425$.

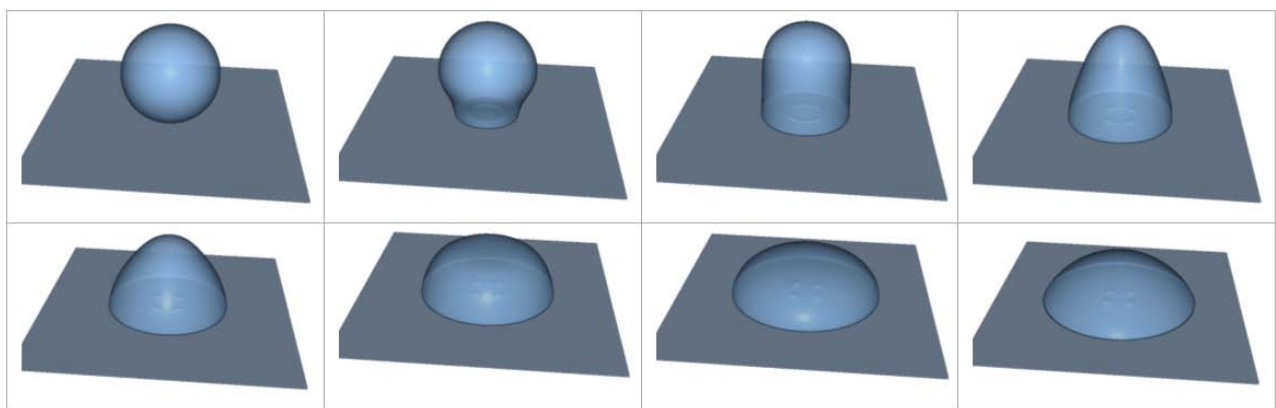


Figure 4. Spreading of a spherical drop with 30 lattice sites radius on a homogeneous surface. In this case, the interaction factor is equal to 0.82 resulting in an equilibrium contact angle equal to 59.5° .

5.3 Variation of the exponent n with the wettability

Besides the initial condition dependence, it is noticed that the wettability variation is accompanied of a substantial change of n value, presenting negative values for hydrophobic surfaces (not wettable), in which the drop retracts, and growing in way approximately lineal with the contact angle decrease (in other words, with the increase of the interaction factor).

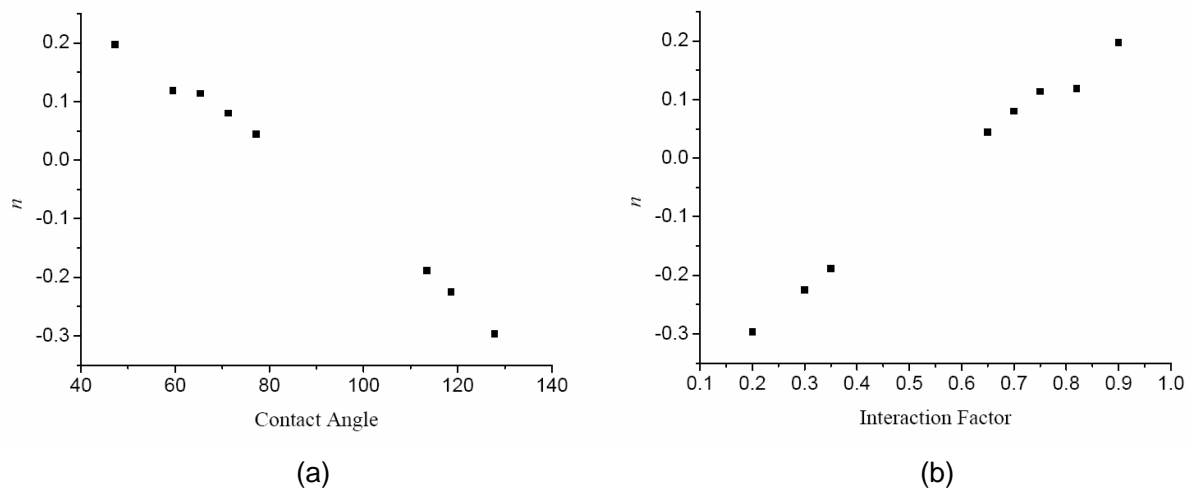


Figure 5. Variation of the exponent n in function of (a) equilibrium contact angle and (b) interaction factor.

5.4 Spreading on heterogeneous surfaces

In real situations it is common that solid surfaces contain physical or chemical heterogeneities. These heterogeneities provoke disturbances in the contact line dynamics during the spread. It has recently become feasible to fabricate surfaces with well-defined chemical properties on micron length scales and it is becoming possible to perform well-controlled experiments which probe the behaviour of mesoscopic droplets on chemically and physically heterogeneous substrates. Thus it is particularly interesting to develop techniques to model the effect of these surfaces on the spreading properties of a droplet. (Dupuis, 2003) In this section it was studied the chemical effect from heterogeneities on the spreading dynamics. To simulate situations in that the surface presents areas that are composed by different materials, or presents some pollutant type, different wettabilitys are attributed on the surface. The analysis will be based on the observation of three different cases, presented in the following sections.

5.5 Solid surface formed by parallel strips with different wettabilitys

In this case, the surface is divided in strips having two different wettabilitys. Sharply, the drop disperses preferentially on the strips with greatest wettability. Figure 6 displays the contact line evolution with the time and the referred preferential displacement. It is also noticed that the spreading on each strip is influenced by the neighboring strip. This influence is also verified when drop sections are analyzed on different surface strips. With the angles measurement method adopted, the following contact angles are obtained: 63.6° in position $x = 71$ that corresponds to the central line of a strip with interaction factor 0.6 and 61.2° in $x = 79$, central line of a strip with interaction factor equal to 0.9. The equivalent equilibrium angles for a homogeneous surface having those same interaction factors are 83.0° and 47.2° respectively. They are represented in the left part of Fig. 7, and the measured values are shown in the right part of the same illustration. This demonstrates a mutual and intense influence of both areas on the equilibrium contact angle. When the images of the sections used in the measures are analyzed, it is noticed that for a region close to the substratum, the contact angles approach the values found for homogeneous surfaces (see Fig. 7). These angles are not detected by the used method, because it bases on a circular approach for the drop section and it measures the contact diameter in a position $z = \delta$ above the solid surface, as discussed previously.

5.6 Solid surface formed by sites with two wettabilitys, random distributed

A solid surface is formed by sites that presents one of the selected wettabilitys, randomly dispersed. In this case each surface site assumes the interaction factor of 0.7 or 0.9. It is Observed that the contact line moves more quickly on those areas that present highest density of sites with high wettability. However, as the wettabilitys distribution is randomic, not presenting preference for a specific wettability, the spreading dynamics is similar to that on homogeneous surfaces. The drop disperses staying in the central domain area, maintaining the contact line approximately circular. This allows the same analysis used for the homogeneous surfaces. However, to guarantee a better approach for the medium contact area radius (R) assuming a circular approach, it is calculated based in the contact area (A) between drop and solid, and is given by $R = (A/\pi)^{1/2}$. Is considered contact area, the number of sites immediately above the solid that present $\rho_R > \rho_B$. So, it is obtained for the described situation, the exponent $n = 0.11 \pm 0.0008$. It can be noticed that n tends to the value

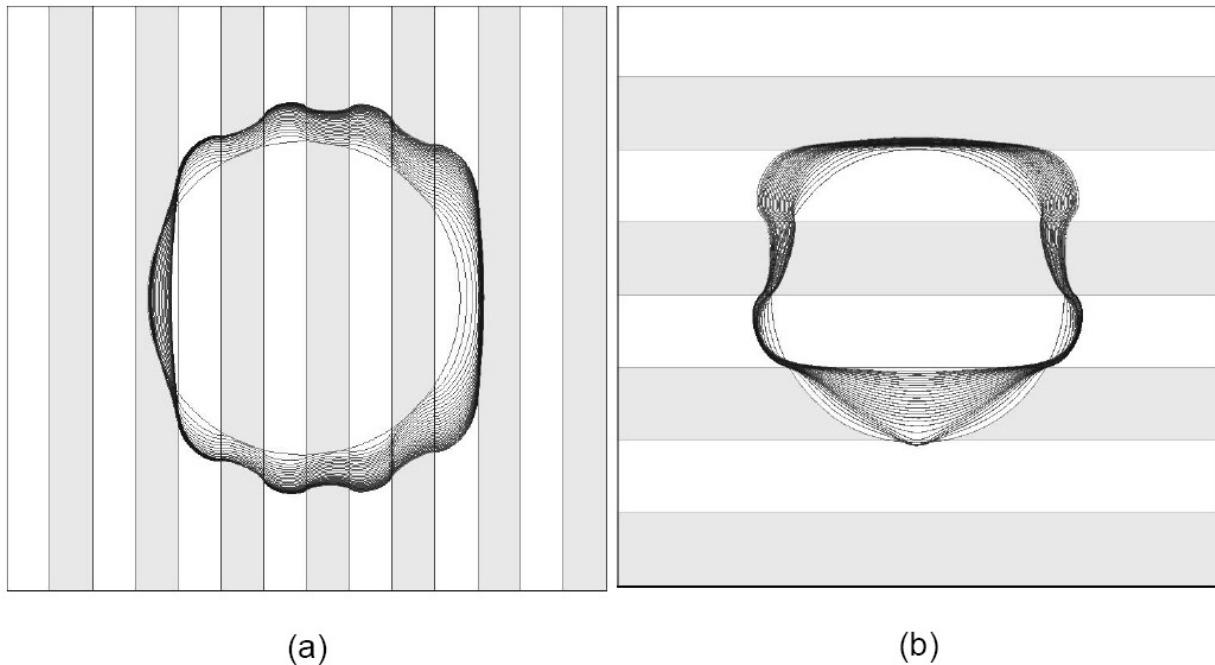


Figure 6. (a) Contact line evolution on a surface divided in strips with interaction factor of 0.6 (grey stripes) and 0.9, with width equal to seven lattice sites. (b) Same to the item (a) for strips width equal to fifteen lattice sites.

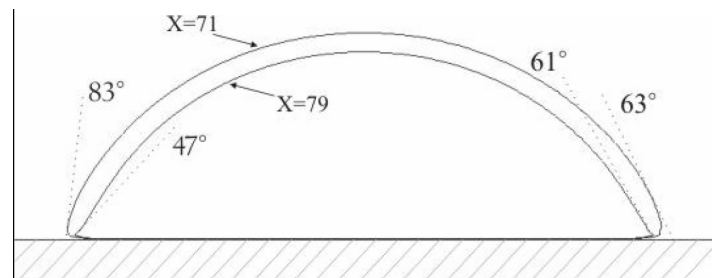


Figure 7. In the right side, contact angles measured on the central lines of two strips with different wettabilitys (positions $X = 71$ and $X = 79$) in the equilibrium situation. At left, the equilibrium angles measured in homogeneous surfaces with the respective wettabilitys, are represented.

corresponding to a surface with interaction factor equal to the average the used factors, as the case shown in the beginning of the section.

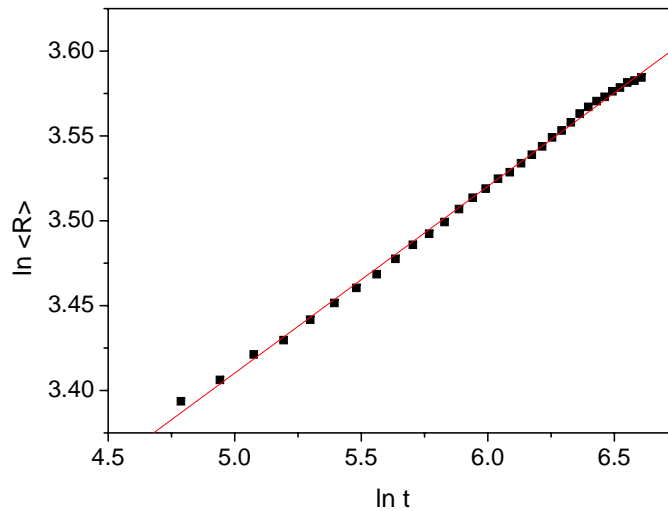


Figure 8. $\ln R \times \ln t$ graph for a drop spreading in condition (a), on a heterogeneous surface with interaction factors equal to 0,7 and 0,9. The resulting angular coefficient is .

5.7 Squared surface with different wettabilitys

The solid surface is divided in equilateral squares, being attributed to each square an interaction factor chosen randomly in a defined interval $[0.7; 0.9]$. Once the wettabilitys distribution (interaction factors) is uniform in the interval, each value of interaction factor has equal probability of being found in the solid. The smallest possible variation among two factors was adjusted for 0.01. In the same way that in the previous cases, the drop movement feels preferentially on the surface regions that present larger interaction factor (in other words, smaller contact angle) average. When the square area is small in relation to the final drop-solid contact area, the dispersal speed variations are small, still allowing the movement characterization through proportionality law $R \propto t^n$. In this cases it can be noticed that the n value found is between the values corresponding to homogeneous surfaces ($n = 0.0804$ for interaction factor 0.7 and $n = 0.1972$ for interaction factor 0.9). As the squares areas increases the drop dispersal is more influenced, presenting speed and direction variations along the time (Fig 9).

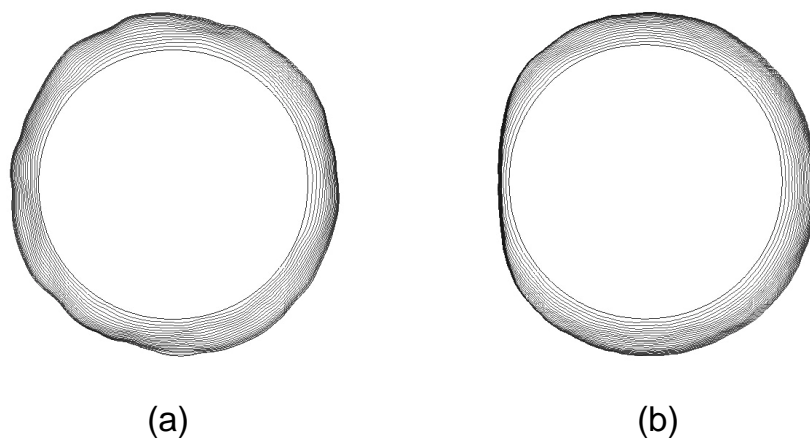


Figure 9. Contact line evolution for a drop dispersing on a heterogeneous surface divided in (a) 4 lattice sites squares and (b) 7 lattice sites squares (interaction factors between 0.7 and 0.9).

Figure 11 shows the contact line dynamics formed by a drop on a very heterogeneous surface. It is noticed that dispersing is always followed by drop retraction. This dynamics type illustrates the intermittent drop movement in which

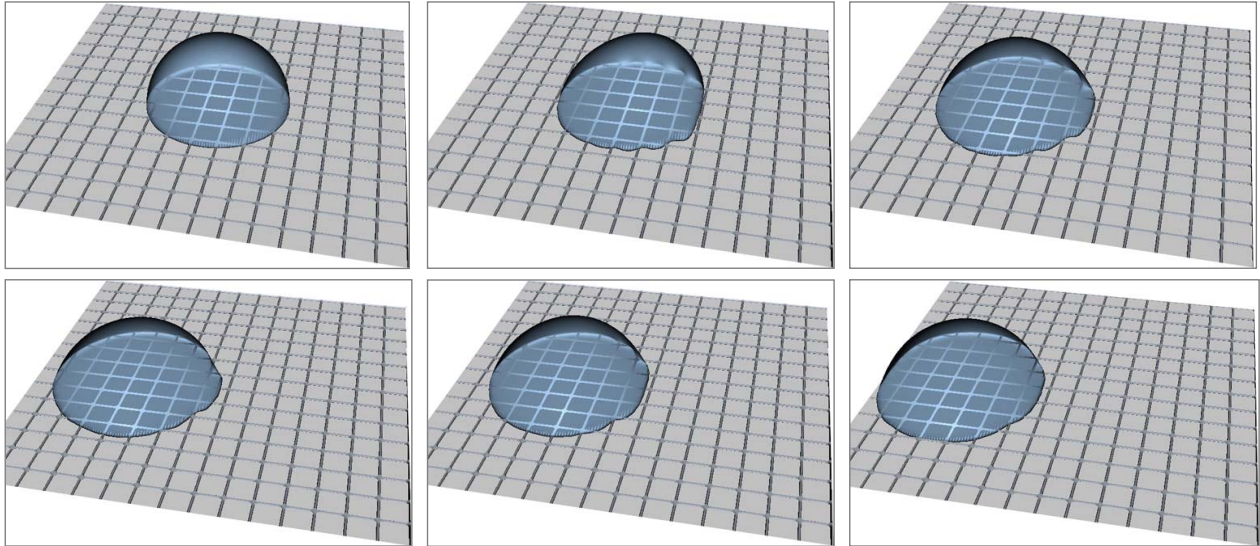


Figure 10. Drop spreading on a heterogeneous squared surface. Wettability values between 0.7 and 0.9 and squares with 10×10 lattice sites.

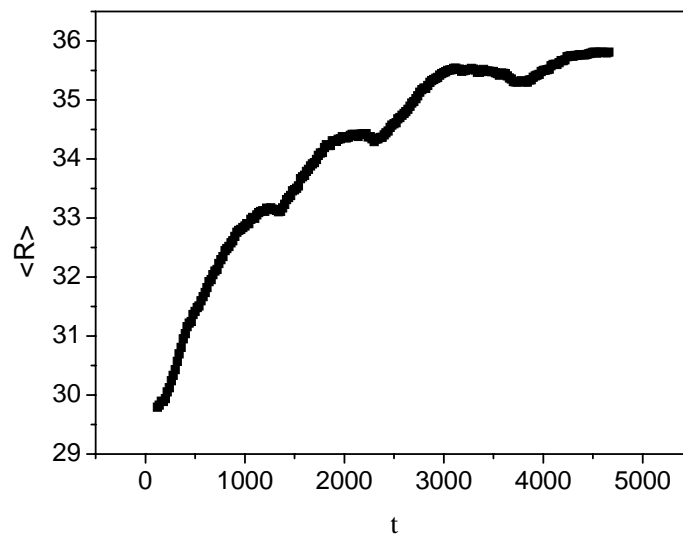


Figure 11. Radium average evolution of the drop contact area on a heterogeneous surface divided in 10×10 lattice sites squares.

a part of the contact line becomes momentarily fixed in areas with smaller wettability, while it continues moving onto larger wettability areas. This behavior is similar to the contact line pinning in presence of surface irregularities.

6. Conclusion

The model developed by Santos and Philippi (2003) used in this study allows to simulate, in static and dynamic conditions, drops in contact with a substrate and its movement on homogeneous and heterogeneous surfaces. The model is capable to simulate dynamic effects among drop and surface, presenting satisfactory results when compared with the literature for homogeneous surfaces. This qualifies it as a powerful tool for investigation of factors that affect the drops dynamics on a substrate, as initial condition, contact angle and surface heterogeneities. These heterogeneities are represented through a local surface wettability variation and influence the contact line dynamics, altering the drop spreading speed and producing fixation phenomena (pinning) in certain areas. There are situations in that these irregularities can move the drop for relatively big distances. The contact angles in the heterogeneity place tend to the characteristic value of its wettability, however they are also influenced by the wettability of its neighborhood. The proportionality law coefficient n in surfaces with great wettability variation acquires average values among homogeneous surfaces n values. Other studies on the initial conditions, physical heterogeneities and their influences on drops spreading speed should be developed, to represent more faithfully practical situations and determine the model applicability.

7. Acknowledgements.

The authors would like to acknowledge CENPES/ PETROBRAS (Centro de Pesquisas e Desenvolvimento Leopoldo A. Miguez de Mello) for providing the images and the experimental data for reservoir rocks. The authors also acknowledge the financial support of CNPq (Conselho Nacional de Desenvolvimento Científico e Tecnológico), ANP (Agência Nacional do Petróleo) and FINEP (Financiadora de Estudos e Projetos).

8. References

- Santos, L.O.E., Facin, P.C., Philippi, P.C., 2003, "Lattice-Boltzmann model based on field mediators for immiscible fluids", *Physical Review E*, vol. 68 No. 5, Art. No. 056302.
- Succi, S., 2001, "The Lattice Boltzmann Equation for Fluid Dynamics and Beyond", Oxford University Press, Oxford.
- Qian, Y. H., d'Humieres D., Lallemand P., 1992, "Lattice BGK Models for Navier- Stokes Equation", *Europhys. Lett.* 17, pp. 479-484.
- Dupuis, A., Briant, A.J., Pooley, C.M. and Yeomans, J.M., 2003, "Droplet Spreading on Heterogeneous Surfaces Using a Three-Dimensional Lattice Boltzmann Model" *Lecture Notes in Computer Science* 2657, pp. 1024-1033.
- Blake, T.D., De Coninck, J., 2002, "The influence of solid-liquid interactions on dynamic wetting" , *Advances in Colloid and Interface Science*, vol.96, pp. 21-36.
- Cazabat, A. M., 1987, "How does a droplet spread?" *Contemp. Phys*, vol. 28, no. 4, pp. 347-364.
- Dussan, V. E. B., 1979, "On the spreading of liquids on solid surfaces: static and dynamic contact-lines" *Annual Rev. Fluid Mech.* vol. 11, pp. 371.
- De Coninck J, de Ruijter M.J. and Voue M., 2001, "Dynamics of wetting", *Current Opinion in Colloid and Interface Science*, vol. 6, no. 1, pp. 49-53.
- Liu, Y. German, R. M., 1996, "Contact Angle and Solid-Liquid-Vapor Equilibrium", *Acta Mater*, vol. 44, pp. 1657.
- Marmur, A., 1983, "Equilibrium and Spreading of Liquids on Solids Surfaces", *Advances in Colloid and Interface Science*, vol. 19, pp. 75-102.
- Lelah M.D. and Marmur A., 1981, "Spreading Kinetics of Drops on Glass" vol.82, no. 2, pp. 518-525.
- Cubaud,T., Fermigier, M. and Jenffer, P., 2001, "Spreading of Large Drops on Patterned Surfaces", *Oil and Gas Science and Technology*, Vol. 56, No. 1, pp. 23-31.

9. Responsibility notice

The author(s) is (are) the only responsible for the printed material included in this paper